UC San Diego
UC San Diego Electronic Theses and Dissertations

Title

Sex Differences in Type-2 Diabetes: Caveolin-3 Protects a Diabetic Heart

Permalink

https://escholarship.org/uc/item/4z5124dr

Author

Ronquillo, Antoinette

Publication Date

2020

Peer reviewed|Thesis/dissertation

UNIVERSITY OF CALIFORNIA SAN DIEGO

Sex Differences in Type 2 Diabetes: Caveolin-3 Protects a Diabetic Heart

A thesis submitted in partial satisfaction of the requirements
for the degree Master of Science

in

Biology

by

Antoinette Ronquillo

Committee in charge:

    Professor Hemal Patel, Chair
    Professor Sonya Neal, Co-Chair
    Professor Kimberly Cooper

2020

The thesis of Antoinette Ronquillo is approved, and it is acceptable in quality and form for publication on microfilm and electronically:

_____

_____

Co-chair

_____

Chair

University of California San Diego

2020

DEDICATION

I dedicate this thesis to my grandmother,

Purificacion Hooten, and to my mother,

Janette Ronquillo, for their empowerment

and unconditional love.

EPIGRAPH

I learned that courage was not the absence of fear, but the triumph over it.
The brave man is not he who does not feel afraid but he who conquers that fear.

Nelson Mandela

TABLE OF CONTENTS

LIST OF FIGURES

LIST OF TABLES

ACKNOWLEDGEMENTS

I would like to thank Dr. Hemal Patel for his guidance and support during my time as an undergraduate and graduate student working in his lab. The advice and direction that he has provided me as my principal investigator and committee chair has been invaluable throughout this whole process. I am grateful that he has entrusted me to be a part of such a thrilling project.

I am truly grateful for meeting Dr. Alice Zemljic-Harpf. To begin, I acknowledge her expertise in cardiology and her technical contributions of echocardiography towards this study. Her constant support as my advisor and mentor has shaped who I am today as a woman in STEM. She has devoted her time to teach me various techniques and aspects of professionalism that I will hold onto forever. I idolize her conviction and passion for research and hope to have that same sense of motivation in my future.

I would like to thank the Cardiac & Neuro Protection Lab team members Marianne Thio, Mehul Dhanani, and Joseph Leem for making lab enjoyable and providing their tireless efforts towards this project.

In addition, I would like to thank Dr. Sonya Neal and Dr. Kimberly Cooper for joining my committee and providing their insight and moral support. These two women are truly inspiring.

The results are unpublished and coauthored with Zemljic-Harpf, Alice E.; Dhanani, Mehul; Leem, Joseph S.; Thio, Marianne P.; Alas, Basheer F.; Kim, So Yeon; Schilling, Jan M.; Roth, David M.; Patel, Hemal H. Antoinette Ronquillo was the primary author of this paper.

ABSTRACT OF THE THESIS

Sex Differences in Type-2 Diabetes: Caveolin-3 Protects a Diabetic Heart

by

Antoinette Ronquillo

Master of Science in Biology

University of California San Diego, 2020

Professor Hemal Patel, Chair
Professor Sonya Neal, Co-Chair

The rise of type 2 diabetes (T2DM) increases the risk of diabetic cardiomyopathy. Worsened cardiovascular outcomes have been clinically observed in female diabetic patients; however, there is a lack of sex specific treatments for diabetes associated heart complications. Caveolins are integral membrane proteins expressed in caveolae and mitochondria that act as cellular signaling platforms to regulate stress responses.

The cardiac-specific caveolin-3 overexpression (Cav3 OE) has been shown to protect the heart from morphological changes induced by stressors and preserve mitochondrial function, but this has not yet been shown in a diabetic heart. We tested the rationale that Cav3 will protect the heart from diabetes-induced metabolic injury and be especially advantageous for females. Mid-aged male and female Cav3 OE mice and transgene-negative (Tg-Neg) littermates were either injected with streptozotocin (STZ) and fed a 60% kcal high-fat diet (HFD) to induce diabetes or injected with citrate buffer and fed a 4% kcal low-fat diet for controls. STZ/HFD significantly increased weight and impaired glucose tolerance of male and female mice, with worsened glucose tolerance in males. Tg-Neg T2DM mice presented cardiac hypertrophy in males and females, mitochondrial dysfunction in females, diastolic dysfunction in males, and cardiac mitochondrial disarray in males and females. Meanwhile, Cav3 OE prevented these incidences in T2DM mice. Therefore, Cav3 may be a novel target to protect diabetic mice, especially females, from cardiac complications.

INTRODUCTION

The current obesity epidemic is a severe public health crisis in America (Office of the Surgeon General (US), 2001). In 2015, the prevalence of obese adults in America was nearly 40%, which translates to about 93.3 million people (Hales *et al.,* 2015). Obesity is associated with an increase in body mass and weight gain, which heightens the risk of diabetes. The risk of type 2 diabetes (T2DM) is increased by 7 fold among obese individuals (Abdullah *et al.,* 2010)**.** According to the Centers for Disease Control and Prevention in 2015, there were 30.3 million Americans diagnosed with diabetes and 84.1 million Americans designated to have pre-diabetes (Centers for Disease Control and Prevention [CDC], 2017). Additionally, approximately 463 million adults lived with diabetes worldwide in 2019, which is projected to rise to 700 million by 2045 (International Diabetes Federation, 2019).

Diabetes is a chronic health condition that results from the inability of the body to process blood glucose (Palicka, 2002). After a meal, glucose becomes present in the blood and pancreatic beta cells are stimulated to release the hormone insulin (Komatsu *et al.*, 2013; Strubbe and Steffens, 1975). Free insulin interacts with membrane bound glycoprotein receptors located within surrounding insulin sensitive tissues, activates a downstream signaling cascade, and triggers the uptake of circulating glucose (Kahn, 1985). Glucose is then utilized by numerous cells to carry out cellular functions or to store for later use. If left unmanaged, diabetes may result in organ damage or failure in the eyes, kidneys, nerves, blood vessels, and heart (Mayo Clinic, 2018). Among all of these complications, the leading cause of death in those with diabetes is due to cardiovascular disease (Raghavan et al., 2019). For non-diabetic individuals, the risk of

cardiovascular disease is higher in men than women; however, for those with diabetes, women are at a 44% greater risk of cardiovascular disease compared to men (Kannel & Wilson, 1995; Peters *et al.*, 2014). Diabetic women also have a 50% higher risk for fatal heart complications than diabetic men (Huxley *et al.,* 2006). Therefore, this pathophysiological relationship between diabetes, sex, and the heart must be addressed for improved diagnosis, therapy, and prevention of diabetes-induced heart disease.

In some cases, individuals are either insulin deficient or their cells have a poor insulin response, which results in hyperglycemia or high blood glucose levels (Wilcox, 2005). There are two broad classes of diabetes, type 1 and type 2. Type 1 is characterized as absolute insulin deficiency, due to an immune-associated destruction of insulin-producing pancreatic beta cells, causing a state of insulin deficiency (Atkinson *et al.*, 2014). Without sufficient beta cells, the pancreas is unable produce insulin to stimulate the uptake of glucose, resulting in high plasma glucose levels or hyperglycemia (Atkinson *et al.*, 2014). This chronic disease only affects 5-10% of the diagnosed diabetic population and is most prevalent in children (American Diabetes Association, 2010). Type 2 diabetes most commonly results from obesity, due to chronic inflammation from the expansion of adipose tissue (Dandona *et al.,* 2004). Type 2 diabetes is a metabolic disorder associated with the resistance of free insulin by insulin receptors on the surface of cells (Wilcox, 2005). This results in high blood glucose, which can lead to various health complications and induce type 1 diabetes. Type 2 diabetes accounts for 90 to 95% of all diagnosed diabetes cases in adults (American

Diabetes Association, 2010) and unfortunately leads to very severe health complications.

As previously mentioned, cardiovascular disease is the leading cause of death among diabetic patients. There are various forms of cardiovascular diseases induced by diabetes; however, cardiomyopathy is the most prevalent (Battiprolu *et al.*, 2010; Witteles and Fowler, 2008). During diabetes, high-blood glucose levels (hyperglycemia) and insulin resistance induce metabolic damage, oxidative stress, and mitochondrial dysfunction. In turn, these disorders accelerate the progression of diabetes-induced cardiomyopathy (Maritim *et al.*, 2003). Cardiomyopathy is a heart muscle disorder, which in serious cases can result in an inefficiency of blood pumping from the heart and eventually lead to heart failure (Jia *et al.*, 2018). The heart is dense in mitochondria because it requires excessive amounts of energy to meet its metabolic demand, therefore, mitochondrial damage harms the heart. (Ventura-Clapier *et al.*, 2011)**.** Two hallmarks of diabetic cardiomyopathy include diastolic dysfunction and changes in morphology (Boudina & Abel, 2010; Meyers *et al.*, 2013).

Disruption of cardiac morphology, indicated by left ventricle hypertrophy, and abnormal diastolic and systolic cardiac function are characteristics of cardiomyopathy (Jia *et al.,* 2018). In a state of hypertrophy, the heart enlarges, its muscles thicken, and its chambers become smaller, which weakens the heart's ability to pump blood throughout the body (Kavazis, 2015). In turn, this phenotype disrupts cardiac function as the heart is required to work harder to pump blood throughout the rest of the body and maintain cardiac output. These complications can worsen and eventually lead to heart failure, arrythmias, rapid heartbeat, ischemia (reduced oxygen supply to the heart),

stroke, and cardiac arrest (Mayo Clinic, 2018). In regard to sex differences, since

diabetic women have greater risk for more severe cardiac outcomes compared to

diabetic men, this suggests a worsened path towards diabetic cardiomyopathy and

heart failure. While lifestyle changes are necessary to prevent type 2 diabetes and

reduce heart complications, more robust treatments are needed to protect those who

are already at risk.

The most commonly used treatments for diabetic patients include blood glucose

controlling drugs; however, these methods do not always prove to be advantageous for

the heart (Marín-Peñalver *et al.*, 2016). Current glucose-lowering drugs are not aimed at

protecting the diabetic heart and do not improve the number of heart failure

hospitalizations among diabetic patients (Castagno *et al.*, 2011). For example,

Rosiglitazone was developed as an anti-diabetic drug to sensitize cells to insulin and

lower amounts of blood glucose; however, it was correlated with a high risk of heart

attack and death and removed from the market (Nissen and Wolski, 2007). Despite the

differences in the pathophysiology of diabetes and heart disease among men and

women, most diabetes studies do not consider the impact of sex differences on the data

(Legato et al., 2006). Additionally, most clinical diabetes studies have focused on men

and treatment and prevention methods are identical for men and women (except

pregnant women), which calls for a more personalized gender approach (American

Diabetes Association, 2014).

Aside from drugs, gene therapy seems to be an appropriate method for treating

diabetes induced heart complications (Borghetti *et al.*, 2018). As briefly mentioned, the

diabetic state is closely related to mitochondrial dysfunction, which heightens the risk of

heart complications. Therefore, the Hspa9 gene in mice, that encodes mitochondrial heat shock protein 70 (HSP70) is a gene target of interest (Shepherd *et al.*, 2018). Nearly all mitochondrial proteins are imported into mitochondria from the nucleus by mtHsp70 (Shepherd *et al.*, 2018). Type 2 diabetes has shown to manipulate the function of mtHsp70 by decreasing protein import into mitochondria, disrupting the makeup of mitochondrial proteomes, and impairing normal mitochondrial function (Shepherd *et al.*, 2018). Shepard*,* revealed that the cardiac-specific overexpression of mtHsp70 in transgenic, diabetic mice restored protein import and mitochondrial and cardiac function (Shepherd *et al.*, 2018). Since mtHsp70 gene therapy has displayed cardio protection in diabetic mice, gene targets for combating diabetic cardiomyopathy are being explored, including the caveolin gene family.

The caveolin gene family consists of CAV1 encoding caveolin-1, CAV2 encoding caveolin-2, and CAV3 encoding caveolin-3 (Williams and Lisanti, 2004). Caveolins behave as a scaffold for cellular signaling molecules within lipid raft structures known as caveolae (Sargiacomo *et al.*, 1995). Caveolae were first discovered in 1953, by biologist George Palade. Palade noticed small bulb-shaped curvatures in the plasma membrane of endothelial cells in the heart and named them "plasmalemmal vesicles" (Palade, 1953). Two years later these vesicles were renamed "caveolae intracellulares" by Enichi Yamada due to their similarity of caves (Yamada, 1955). Caveolae are present in the plasma membrane and their formation requires caveolin proteins (Fra *et al.,* 1995). Caveolin-1 and -2 proteins are present in multiple cells, whereas caveolin-3 is expressed only in striated muscle types, specifically cardiac muscle (Tang *et al.*, 1996). Caveolin-3 is a structural protein that localizes in various cellular compartments and

organelles, such as the plasma membrane and mitochondria (Fig. 1) (Schilling and Patel, 2016).

Caveolin-3 has a protective role in the heart and cardiac mitochondria (Fridolfsson et al., 2012; Horikawa et al., 2011). In a caveolin-3 knockout study in mice, the caveolin-3 knockout hearts displayed abnormal cardiac function and cardiomyopathy (Woodman *et al.*, 2002). Another caveolin-knockout study in mice displayed abnormal mitochondrial function and increased production of highly destructive reactive oxygen species (Fridolfsson *et al.*, 2012). Meanwhile, the overexpression of caveolin-3 in cardiomyocytes in mice subjected to a surgery that induced heart failure attenuated cardiac hypertrophy, maintained cardiac function, and increased survival (Horikawa *et al.*, 2011). The mitochondria of caveolin-3 overexpressing cardiomyocytes displayed enhanced respiratory function, improved mitochondrial structure, decreased apoptotic stress, and reduced cardiac damage (Fridolfsson *et al.*, 2012). These studies display the promising features of caveolin-3; however, they fail to investigate if the role of caveolin-3 is specific for male or female mice. Therefore, it is uncertain if caveolin-3 protects a male and female heart differently.

Existing studies have clearly established that caveolin-3 has the ability to rescue abnormal cardiac and mitochondrial function; however, the role of caveolin-3 in diabetes-induced mitochondrial and cardiac damage has yet to be investigated. Additionally, and the worsened cardiac outcomes in females suggest that females need additional cardio-protection. The goals of this project are to investigate the ability of caveolin-3 to rescue a male and female diabetic heart and survey its potential as a novel gene therapy. Therefore, the overall research question of this project is, what are

the effects of caveolin-3 in a diabetic heart of male and female mice? In order to assess the effects of caveolin-3 overexpression, the pathophysiology of diabetic cardiomyopathy in male and female mice overexpressing caveolin-3 will be studied. Furthermore, since women are experiencing a worsened path to diabetes-induced cardiovascular disease, it is hypothesized that the overexpression of caveolin-3 will protect the heart and especially of females, from diabetes-induced metabolic injury.

In this study, male and female mice will receive an injection of streptozotocin and high-fat diet treatment to induce diabetes, and the pathophysiology of diabetes will be examined. The aims of this study are: i) diagnose diabetes and compare the severity of metabolic syndrome in our male and female mice; ii) assess cardiac function and morphology in our male and female mice; iii) examine mitochondrial function and ultrastructure to identify differences in respiration in our male and female mice; and iv) determine the role of caveolin-3 in the heart of our male and female diabetic mice. Through this study we seek to better understand sex differences in type 2 diabetes, examine the role of caveolin-3 in a male and female diabetic heart, and propose a novel therapy for protecting against diabetic cardiomyopathy.

MATERIALS AND METHODS

Animals

All animals and experimental procedures performed were treated in compliance with the U.S. National Academy of Science Guide for Care and Use of Laboratory Animals. All protocols employed were approved by the Veteran Affairs San Diego Healthcare System Institutional Animal Care and Use Committee. Cardiomyocyte specific caveolin-3 overexpressing (Cav3 OE) male and female mice were purchased from Jackson Laboratories (Bar Harbor, ME, USA), delivered at 8 weeks old, and maintained in house. Transgene-negative (Tg-Neg) male and female siblings in the C57BL/6 background were controls.

Type 2 Diabetes Mouse Model

11 to 14-month-old male and female Cav3 OE and Tg-Neg mice were used for this study. Mice designated for diabetes (T2DM) from either genetic background were immediately switched on to a 60% kcal high-fat diet (TD 6414) after being injected with a single dose of streptozotocin (non-fasted, 75mg/kg in citrate buffer 0.1 mol/L, pH=4.5). Streptozotocin is a clinically used chemotherapeutic compound for pancreatic beta cell carcinomas. Streptozotocin accumulates in pancreatic beta cells through the GLUT2 glucose transporter in the plasma membrane, exerts toxic effects towards it insulin-producing activity, and exacerbates pancreatic cell death (Lenzen, 2008). Mice designated as non-diabetic controls (Ctrl) from either genetic background were placed on a standard chow, 4% kcal low-fat diet (TD 7001) after a control injection of citrate buffer (0.1 mol/L). All animals were kept on a 12-hour light-dark cycle in a temperature-

8

controlled room. The study maintained the following 8 groups of mice: males - Tg-Neg Ctrl, Cav3 OE Ctrl, Tg-Neg T2DM, and Cav3 OE T2DM and females - Tg-Neg Ctrl, Cav3 OE Ctrl, Tg-Neg T2DM, and Cav3 OE T2DM. The mice were kept on their respective diet throughout the study. Food intake was monitored weekly and body weights were measured bi-weekly.

Glucose tolerance test (GTT)

At 3 to 4-months post diabetes induction, glucose tolerance tests were performed. Mice were fasted for 11 hours and blood glucose was collected by tail-end cuts. Mice received in intraperitoneal injection of glucose (1 g/kg in 0.9% NaCl), and blood glucose was assayed at 30, 60, 90, 120, and 180 minutes after glucose injection using BAYER Breeze 2 Glucose Meter (Bayer Healthcare LLC, Mishawaka, IN, USA).

Echocardiography

At 5-months post diabetes induction, *in vivo* cardiac function and structure were monitored by echocardiography. Noninvasive transthoracic echocardiography was performed using a small animal, high resolution Vevo2100 imaging unit (Fujifilm VisualSonics Inc., Toronto, Ontario, Canada) with a 17.6 MHz ultrasound probe. ECG was monitored continuously on mice under isoflurane (1-3%) anesthesia maintained on a heated platform.

M-mode measurements were captured to determine the size of the myocardial walls as they contract during systole and relax in diastole. Markers of left ventricular hypertrophy include left ventricle wall thickness (LVPWd), left ventricle mass (LV-Mass),

9

and interventricular septum wall thickness (IVSd). Doppler measurements were recorded to determine blood flow. Systolic cardiac function was assessed by blood ejection patterns. Ejection fraction (%EF) measures the amount of blood released per contraction normalized to the size of the left ventricle (Fonarow & Hsu, 2016). In anesthetized mice, a normal %EF is between 50-75% (Yang *et al*., 1999), while anything below 50% signifies decreased myocardial contractility and indicative of heart failure. Diastolic cardiac function is examined by mitral valve filling pressures. Blood flow from the left atrium, through the mitral valve (MV), and into the left ventricle is measured in early filling E waves (E) and late atrial filling A waves (A). Diastolic function is assessed by MV E/E' ratio. E' is a measure of the velocity of the left ventricle muscle during active relaxation of the left ventricle. A lower ratio indicates improper filling of the LV by slow blood flow and stiffer left ventricle muscle.

Organ Harvest

After 6 months post-diabetes induction, mice were sacrificed, and their organs and tissues were harvested for analysis. The heart, liver, and lung from each mouse were harvested and weighed. The tibia was also removed and measured from each corresponding mouse. To effectively compare organ mass across different animals among the groups, they were normalized for reliability. Body weight is an unreliable measurement for normalization because it fluctuates in old mice. However, tibia length does not change after maturity, proving to be a more reliable measurement for normalization (Yin *et al.,* 1982).

High-Resolution Mitochondrial Respirometry

An Oroboros Oxygraph-2k (Oroboros Instruments, Innsbruck, Austria)

respirometer was used to evaluate mitochondrial respiration. Within the inner

membrane of mitochondria, ATP is formed through the process of oxidative

phosphorylation (OX), which involves the transfer of electrons across a series of protein

complexes from *NADH* or *FADH2* to *O2* (Berg *et al.,* 2002). OX is a coupled state as

ADP phosphorylation is coupled with a proton gradient. To assess mitochondrial

function, different OX substrates and inhibitors are injected into the O2k chamber and

mitochondrial oxygen flux rates are measured. Oxygen flux signifies the rate of

respiration, which is the ratio between ATP production and oxygen consumption. These

rates can be used to conclude details about mitochondrial function, such as respiratory

capacity, integrity, and metabolism (Gnaiger, 2014).

The heart relies on beta/fatty acid oxidation (FAO) as the primary mechanism for

energy metabolism. FAO is another metabolic pathway in mitochondria, similar to OX,

which breaks down fatty acids into cellular energy. Depending on extracellular

conditions and nutrient availability, the heart can switch to different substrates, such as

glucose for OX and fatty acids for FAO.

A Substrate-Uncoupler-Inhibitor-Titration (SUIT) protocol was applied for OX

analysis and examination of respiratory control. Substrates were added at saturating

concentrations to measure respiratory capacity. To achieve a maximum rate of

respiration, titration of the following complex I (CI) and II (CII) substrates occurred

sequentially: glutamate and malate, ADP, cytochrome c, pyruvate, succinate. Next,

FCCP was added to uncouple respiration and ATP synthesis to estimate the maximal

activity of the electron transport system (ETS) (Gnaiger, 2014). Lastly, two CI & CII

inhibitors, rotenone and antimycin A, are added to distinguish any oxygen consumption

occurring from non-mitochondrial sources. A SUIT protocol was also utilized for FAO

analysis with the addition of different substrates. Titration of the following substrates

occurred sequentially: octanoylcarnitine and malate, ADP, cytochrome c, glutamate,

pyruvate, succinate, FCCP, rotenone, and antimycin A.

Fibers of the left ventricular free wall from mouse hearts were manually dissected

from all groups. Each heart sample weighed between 0.5 to 1.0 mg. The tissue was

incubated in the oximetry chamber. After equilibration, substrates were added in a

stepwise manner. The average maximum oxidative phosphorylation capacity and

maximum uncoupled capacity were determined.

Oxygen flux rates were measured after the addition of substrates with triplicates

for each animal and with n>8 females per group and n>6 males per group. O2 flux were

normalized to mass of protein and baseline oxygen flux rates. All measurements were

performed using DatLab 7 software (Oroboros Instruments, Innsbruck, Austria).

Transmission Electron Microscopy

At 6 months post diabetes induction, left-ventricular free wall cardiac tissues

were manually harvested for ultrastructural analysis during sacrifice. Transmission

electron microscopy was used to view the cardiomyocytes and evaluate mitochondrial

morphology and connectivity. Cardiomyocytes are dense with mitochondria, occupying

more than 30% of its volume, due to the extreme demand for energy from ATP

synthesis in the heart (Ventura-Clapier *et al.*, 2011). Toxic cellular environments can

modify the morphology of mitochondria and the ultrastr

ucture of their membrane. This can affect mitochondrial dynamics and disrupt the

organelle's respiratory functions of the electron transport system (Picard *et al.,* 2013).

Mitochondria contain an outer membrane to separate the organelle from the

surrounding cytoplasm and a highly structured inner membrane which separates the

inter-membrane space from the mitochondrial matrix (Kühlbrandt, 2015). The inner

membrane folds onto itself, forming invaginations called cristae which extend into the

mitochondrial matrix. Cristae are the main site of oxidative phosphorylation for ATP

synthesis as it contains nearly all of the electron transport chain complexes and ATP

synthase (Kühlbrandt, 2015). The density and shape of cristae affects mitochondrial

respiratory efficiency (Cogliati *et al*., 2013).

Small heart tissue pieces were incubated in fixative (2.5% glutaraldehyde, 2%

paraformaldehyde in 0.15M cacodylate buffer) for 2 hours at room temperature

immediately after dissection. These samples were followed by overnight incubation at

4°C in the same fixative. The heart samples were post-fixed in 1% OsO_4 in 0.1 M

cacodylate buffer and enbloc stained with uranyl acetate (2%−3%) and dehydrated in

ethanol. For imaging, the samples were embedded in a longitudinal orientation in

Durcupan epoxy resin (Sigma-Aldrich, St. Louis, MO, USA) and polymerized for 48

hours at 60°C. The blocks were sectioned at 50–60 nm on a Leica UCT ultramicrotome

(Wetzlar, Germany), picked up on Formvar and carbon-coated copper grids, and

stained in uranyl acetate and lead citrate (Jeol 1200 EX-II; Jeol Ltd., Akishima, Japan).

Blinded by groups, the tissues were scanned at 2900x, 6800x, and 9300x

magnifications using a Tecnai G2 Spirit BioTWIN (FEI, Hillsboro, OR, USA)

transmission electron microscope. On average, N=6 for female from all groups and N=2

for males from all groups. Images were captured using an Eagle 4k CCD HS digital

camera (FEI, Hillsboro, OR, USA).

Statistics

Statistical analysis of all data was performed using GraphPad Prism 7 software

(GraphPad Software, Inc., San Diego, CA, USA). All data are presented as means ±

SEM. Statistical analysis was assessed using one-way and two-way analysis of

variance (ANOVA) with Tukey tests for multiple comparisons. $P<0.05$ was considered to

be statistically significant.

RESULTS

Streptozotocin Injection and High-fat Diet Increased Body Weight of Middle-Aged Female and Male Mice

To begin, the type 2 diabetes (T2DM) phenotype was defined among the transgene-negative (Tg-Neg) and caveolin-3 overexpressing (Cav3 OE) mice that received streptozotocin (STZ) injection and high fat diet (HFD) treatment. STZ/HFD diet treatment significantly increased body weight of both male and female Tg-Neg and Cav3 OE, starting at 4 weeks post diabetes induction. The significant increase in body weight persisted for the entirety of the 24-week study (Fig. 2A-B). The control-diet fed mice maintained similar body weights throughout the study. At 24-weeks, the sharp decrease in body weight for the male caveolin-3 overexpressing mice was due to a small n of 2 because most mice in that group were already sacrificed. Throughout the 24-week assessment of body weight progression, there were no striking sex differences from STZ/HFD. Male and female body weights were not statistically compared because differences in weight and size could not be normalized, which does not allow for a reliable comparison.

Streptozotocin Injection and High-Fat Diet Impaired Glucose Tolerance in Middle-Aged Female and Male Mice

To further characterize the diabetic phenotype and analyze the effects of STZ/HFD on metabolism, the initial stages of diabetes-related disorder were characterized by glucose tolerance tests (Fig. 3). The body weight of mice in all groups were simultaneously measured during the glucose tolerance tests to reconfirm

15

significant weight gain. Both male and female T2DM groups were significantly heavier than the male and female control groups. There were no differences in weight between the Tg-Neg T2DM mice vs. Cav3 OE T2DM mice (Fig. 3A).

Impaired blood glucose tolerance was visible in female and male mice. At fasting, female Tg-Neg control mice displayed an average blood glucose concentration of $157.78 \pm 10.78 \frac{mg}{dL}$, which was very similar to Cav3 OE control mice who had an average blood glucose concentration of $159.11 \pm 16.62 \frac{mg}{dL}$. Meanwhile, the female T2DM had slightly elevated glucose levels at fasting compared to the controls. The female Tg-Neg T2DM mice had an average blood glucose concentration of $185.13 \pm 14.09 \frac{mg}{dL}$, which was slightly lower than the average blood glucose concentration of the female Cav3 OE T2DM mice at $205.75 \pm 37.27 \frac{mg}{dL}$. At 30- and 60-minutes post glucose injection, the female Tg-Neg and Cav3 OE diabetic mice displayed glucose tolerance impairment with significantly elevated blood glucose concentrations compared to the controls. Glucose tolerance was rescued among the female diabetic mice starting at 90-minutes post glucose injection as the blood glucose concentrations were still slightly elevated, but insignificantly different, than the controls. By 180-minutes, the glucose concentration of the female diabetic mice subsided to levels similar to the control mice (Fig. 3B). Initially, male Tg-Neg control mice showed slightly elevated fasting blood glucose concentrations compared to the Cav3 OE control mice ($181.44 \pm 7.15 \frac{mg}{dL}$ vs. $165.22 \pm 4.56 \frac{mg}{dL}$). However, the male Tg-Neg T2DM mice displayed lower fasting blood glucose concentrations compared to the male Cav3 OE T2DM mice ($220.11 \pm 7.59 \frac{mg}{dL}$ versus $242.11 \pm 8.79 \frac{mg}{dL}$) (Fig. 3C). At 30-minutes post glucose injection, the male Tg-Neg

control fed mice had significantly greater blood glucose concentrations than the Cav3 OE control fed mice. This trend continued at 60-minutes post glucose injection but dissipated at 90-, 120-, and 180-minutes post glucose injection (Fig. 3C). At all timepoints (30-, 60-, 90-, 120-, and 180-minutes), the male Tg-Neg and Cav3 OE T2DM mice had significantly greater blood glucose concentrations compared to their respective control mice, indicating glucose intolerance (Fig. 3C). At 180-minutes post glucose injection, the male Cav3 OE T2DM mice displayed rescued glucose tolerance; however, the male Tg-Neg T2DM mice average blood glucose concentration was still significantly greater than the male Tg-Neg control mice (Fig. 3C).

Cardiac Morphology and Function was Preserved in Diabetic Caveolin-3 Overexpressing Mice

Cardiac function was assessed by echocardiography 5-months post diabetes induction to investigate the effects of caveolin-3 overexpression on cardiac morphology and function. Both female and male Tg-Neg T2DM mice presented cardiac hypertrophy through evidence of a significantly enlarged left ventricle. The Tg-Neg T2DM average LVPWd was significantly thicker than that of Tg-Neg control mice. The LV-mass of the Tg-Neg T2DM mice was significantly heavier than the corresponding controls. Additionally, the IVSd for the Tg-Neg T2DM mice was significantly thicker than the controls. Female and male Cav3 OE T2DM mice did not display evidence of cardiac hypertrophy (Table 1.1,1.2).

All female and male groups presented preserved systolic cardiac function. There was no significant difference in %EF between female Tg-Neg control or female Tg-Neg

T2DM mice, as well as female Cav3 OE control or female Cav3 OE T2DM mice (Table 1.1). Males also displayed no significant difference in %EF between Tg-Neg control or Tg-Neg T2DM mice, as well as Cav3 OE control or Cav3 OE T2DM mice (Table 1.2).

Diastolic cardiac function was examined in female and male mice. There was no significant difference in MV E/A or MV E/E' between female control and diabetic mice (Table 1.1). Males displayed no significant difference in MV E/A between control and diabetic mice. However, MV E/E' significantly increased in male Tg-Neg T2DM mice compared to the controls. Cav3 OE T2DM males did not display altered MV E/E' (Table 1.2).

Caveolin-3 Cardiac Overexpression Maintained Relative Organ Weights in Female and Male Diabetic Mice

At 6 months post diabetes induction, the mice were sacrificed, and their highly metabolic organs (heart, lung, and liver) were harvested, weighed, and preserved for potential high resolution respirometry, RNA sequencing analysis, histology, and metabolomic assays.

The mass of the heart, liver, and lung normalized to tibia length were positively correlated with the high body weights of the female T2DM mice. Heart/tibia was significantly greater in Tg-Neg T2DM mice compared to the controls, indicative of cardiac hypertrophy. Lung/tibia was significantly greater in Tg-Neg T2DM mice compared to the controls, suggesting fluid accumulation in the lung, indicative of acute respiratory failure. Heart/tibia and lung/tibia were slightly greater but insignificant in the Cav3 OE T2DM mice compared to the controls. Liver/tibia was significantly greater in

both the female Tg-Neg and Cav3OE T2DM mice compared to the corresponding

controls, indicative of fatty liver disease (Table 2.1).

Only heart and liver mass were positively correlated with the high body weight

gain of the male T2DM mice. Heart/tibia and liver/tibia was significantly greater in the

male Tg-Neg T2DM mice compared to the Tg-Neg controls and indifferent in the Cav3

OE T2DM mice vs. the Cav3 OE controls (Table 2.2). There were no significant

differences in lung/tibia between the male diabetic and control mice.

Caveolin-3 Cardiac Overexpression Rescued Mitochondrial Dysfunction in Female

Diabetic Mice

High resolution respirometry was applied to evaluate mitochondrial respiration

and oxygen dynamics of left ventricular heart samples among our high-fat and control

diet fed mice. The effects of caveolin-3 on mitochondrial function were also examined.

After the addition of complexes I & II substrates during oxidative phosphorylation,

mitochondria from female Tg-Neg T2DM mice displayed a significantly greater oxygen

flux compared to mitochondria from Cav3 OE T2DM mice and greater, but insignificant

oxygen flux compared to the control group mitochondria. After the addition of FCCP to

initiate an uncoupled state, the oxygen flux of female Tg-Neg T2DM mitochondria also

increased significantly compared to both the Tg-Neg control and Cav3 OE T2DM

mitochondria (Fig. 4A). After the addition of fatty acid oxidation substrates to initiate fatty

acid oxidation, the oxygen flux rates of the female Tg-Neg T2DM mitochondria were

greater but insignificantly different compared to the control and Cav3 OE mitochondria

(Fig. 4C). There were no notable differences in respiration among the male mice during

oxidative phosphorylation (Fig. 4B) or fatty acid oxidation (Fig. 4D), suggesting abnormal mitochondrial function and rescue by caveolin-3.

Caveolin-3 Overexpression Preserved Mitochondrial Morphology and Membrane Ultrastructure from Effects of Diabetes in Cardiomyocytes

Transmission electron microscopy (TEM) images were taken of cardiomyocytes from left-ventricular heart samples to examine the composition and arrangement of mitochondria. The TEM images of the male and female control mice displayed healthy mitochondria densely packed with strong connectivity in the cardiomyocytes. The mitochondria also exhibited elongated and crisp cristae and a clear double membrane (Fig. 5 A,B). The Tg-Neg T2DM female mice displayed fuzzy double membranes, indicated by arrows, and the cristae were not as well defined as the controls (Fig. 5A). The Tg-Neg T2DM male mice also displayed mitochondrial disarray. The mitochondria had very sparse and hazy cristae indicated by the arrows. The TEM images showed scattered and loosely packed mitochondria, with limited contact sites (Fig. 5B). In both females and males, the Cav3 OE T2DM mice displayed well maintained mitochondria with sharp cristae, obvious double membrane, and strong connectivity.

The results are unpublished and coauthored with Zemljic-Harpf, Alice E.; Dhanani, Mehul; Leem, Joseph S.; Thio, Marianne P.; Alas, Basheer F.; Kim, So Yeon; Schilling, Jan M.; Roth, David M.; Patel, Hemal H. Antoinette Ronquillo was the primary author of this paper.

DISCUSSION

The overall goal of this study was to evaluate the ability of caveolin-3 to protect a male and female diabetic heart and survey its potential as a novel gene therapy for diabetes associated cardiovascular disease. This study shows that caveolin-3 has protective features in the heart and mitochondria, as mentioned in previous studies (Fridolfsson *et al.*, 2012; Horikawa *et al.*, 2011), also applies to diabetes-induced cardiac injury. Moreover, the results confirm the hypothesis that caveolin-3 overexpression plays a role in protecting diabetic mice, especially females, against diabetes-induced metabolic injury.

It is important to consider the age of mice when modeling type 2 diabetes. Diabetes is a disease of older humans, and is usually diagnosed in adults ranging from 45 to 64 years old (Centers for Disease Control, 2017). In order to properly mimic the molecular and morphological features of human T2DM in a mouse model, 11 to 14-month old mice were used in this study to imitate a >50-year-old human. STZ/HFD effectively induced obesity and altered glucose tolerance in mid-aged male and female mice. The mice in this study developed a clear T2DM phenotype and metabolic syndrome indicated by significant weight gain 1 month post (Fig. 1) and impaired glucose tolerance 3 months post diabetes-induction (Fig. 2), which is consistent with previous STZ/HFD-induced T2DM rodent studies (Parikh *et al.,* 2017; Skovsø, 2014). The diabetic males revealed worsened glycemic dysregulation from a more delayed glucose clearance compared to diabetic females. These sex differences in glycemic handling agree with findings from previous studies *(*Chandramouli *et al., 2018;* Pettersson*, et al.,* 2012).

The results demonstrated the caveolin-3 overexpression prevented diabetes-induced cardiac hypertrophy in male and female mice (Table 1). Left ventricle hypertrophy is a hallmark of diabetic cardiomyopathy (Boudina and Abel, 2010). The heart enters a state of hypertrophy in response to chronic stressors like inflammation, oxygen deficiency, and metabolic disorders, in order to preserve contractility and function. Eventually, ongoing stress and hypertrophy can lead to heart failure (Levy et al., 1987). Previous works display Cav3's role in protecting from surgical and drug induced cardiac hypertrophy. The cardiomyocyte specific overexpression of Cav3 protected mice from pressure overload-induced hypertrophy (Horikawa et al., 2011) and angiotensin-II infusion induced hypertrophy (Markandeya et al., 2015). Our results are consistent with these findings and show that the increased expression of caveolin-3 prevents from STZ/HFD-induced cardiac hypertrophy (Table 1).

This phenomenon may be explained by the interaction between caveolin-3 and atrial natriuretic peptide (ANP). ANP is a small peptide that is released by the heart in response to high blood pressure. ANP acts to excrete renal sodium and water to lower blood pressure (Curry, 2005). It has been shown that cardiomyocyte-specific caveolin-3 overexpression enhances ANP expression and signaling in mice (Horikawa et al., 2011). Additionally, mice with pre-existing cardiomyopathy and normal levels of ANP expression displayed better systolic function, increased survival and protection against heart failure, compared to cardiomyopathic mice with reduced or absent ANP expression (Wang et al., 2014). An increase in ANP also prevented cardiac hypertrophy in mice subjected to a transverse aortic constriction surgery that pressurized and enlarged their hearts (Horikawa et al., 2011). Furthermore, there is a causal relationship

22

between low plasma ANP levels and an elevated risk of diabetes (Jujić et al., 2014; Magnusson et al., 2012). Based on these findings, it is possible that the increase of caveolin-3 interacts with ANP and enhances its expression to protect a diabetic heart from cardiomyopathy and heart failure. Therefore, studying the relationship between caveolin-3 and ANP in the pathophysiology of diabetes and associated cardiac complications may be valuable.

The results show that only the Tg-Neg T2DM male mice present diastolic dysfunction by an increased MV E/E' value (Table 1.2). Diastolic function in females was not altered. This finding challenges previous studies which show that STZ-induced diabetic female mice presented diastolic dysfunction through an increased MV E/E' value (Chandramouli *et al.,* 2018). The mice used in Chandramouli were only treated with streptozotocin for diabetes injection without the addition of high-fat diet. This suggests that the effects of glucose overload and stimulated pancreatic beta cell dysfunction may worsen the male diabetic heart. This phenomenon would be interesting to explore in future studies. Obesity and diabetes influences heart failure with preserved ejection fraction, a condition known as HFpEF, which was observed in our Tg-Neg T2DM male mice. During HFpEF, the heart displays a normal ejection fraction and pumps blood normally, but it does not relax and fill with blood properly (diastolic dysfunction) (Zile et al., 2001). Out of all of the heart failure patients in the US, about half present HFpEF, which will continue to rise (Mozaffarian et al., 2015). This statistic reveals the significance of understanding the underlying mechanisms behind HFpEF and other diabetes-induced cardiac complications and evaluating Cav3 as a potential target.

Mitochondria play a critical role in the pathophysiology of diabetes, and caveolin-3 has been shown to preserve mitochondrial function. High blood glucose impairs insulin signaling and alters substrate metabolism, which alters cardiac mitochondrial function (Bugger and Abel, 2010; Dassanayaka *et al.*, 2015). Examination of mitochondria from the hearts of insulin-resistant, Zucker obese rats displayed disrupted morphology with swollen mitochondria and disorganized cristae (Katakam *et al.,* 2007), which is consistent with the observations revealed from TEM in this study (Fig. 5). Mitochondria from the hearts of STZ-induced diabetic rats revealed altered oxygen consumption and oxidative phosphorylation rates (Ferko et al., 2006), which agrees with the abnormal, increased oxygen flux in the female transgene-negative diabetic mitochondria compared to the controls (Fig. 4). Cav3 OE was shown to protect female diabetic mice from both an increased oxygen flux and disrupted mitochondrial ultrastructure. However, the underlying mechanism behind this Cav3 OE protection still requires further investigation.

Increased in oxygen flux translates to a greater influx of oxygen in mitochondria to move electrons across the electron transport system for energy production. An increase in oxygen consumption is generally associated with an increase in ATP production, which is beneficial for more energy available for cellular processes. However, the respiratory assay used in this study failed to measure ATP production. It is uncertain if more oxygen is being used to create more ATP or if the mitochondria are overcompensating their oxygen utilization to synthesize normal levels of ATP. Additionally, the mitochondrial respiratory assays in this study were performed on elderly male and female diabetic mice. It would be insightful to assess the respiratory

capacity of young male and female Tg-Neg and Cav3 OE diabetic mice to determine diabetes-induced mitochondrial dysfunction is age dependent.

The analysis of sex differences was another major component of this study. Sex differences may be caused by sexual hormones, reproductive function, or sex-specific gene expression of autosomes (Regitz-Zagrosek *et al.,* 2016). The transition into menopause increases risk of metabolic diseases, such as obesity, diabetes, cardiovascular disease, and cancer (Stachowiak *et al.,* 2015). It is likely that the female susceptibility of disease may be due to the loss of the protective effects from estrogen. Estrogens play a major role in the causes and consequences of female obesity (Leeners *et al.,* 2017). Estrogens induce the activity of estrogen receptors, which regulates the expression of natriuretic peptides to facilitate the browning of white adipocytes (Palmer and Clegg, 2015). Metabolic activity is decreased in white adipocytes due to mitochondrial uncoupling and increased in brown adipocytes where mitochondrial biogenesis is activated (Bordicchia *et al.*, 2012). The number of brown adipocytes decreases after menopause due to the reduction of estrogens and consequently the downregulation of natriuretic peptides, decreasing metabolic activity. Estrogen receptor alpha (ERa) is the main regulator of energy balance and glucose homeostasis in females (Barros *et al.,* 2006). A global ERa knockout in mice resulted in reduced oxygen consumption, impaired glucose tolerance, skeletal muscle insulin resistance, and inflammation (Ribas *et al.*, 2010). An ERa knockout specifically in skeletal muscle of female mice resulted in mitochondrial dysfunction, lipid accumulation, disrupted mitochondria morphology, and insulin resistance (Ribas *et al.*, 2016).

There is also evidence that ERa interacts with caveolin 3 in the maintenance of cardiometabolic health. Estrogen improves glucose uptake by upregulating caveolin-3. Increased Cav3 expression may be enhancing natriuretic peptide expression to compensate for the loss during aging. Caveolin-3 also transports glucose receptor GLUT4 to the plasma membrane to promote glucose uptake in response to rising blood glucose levels (Tan et al., 2012). It was shown that ERa and Cav3 also co-localize in caveolae on the surface membrane of adult cardiomyocytes. Cav3 acts as a scaffold to dock ERa on caveolae within the plasma membrane (Chung *et al.*, 2009). These previous studies may suggest that the interactions between caveolin-3 and ERa in the female mice of this study is crucial for metabolic homeostasis. As caveolin-3 is primarily expressed in striated muscle types, it is reasonable to suggest that Cav3 interacts with ERa to preserve the metabolic function of female mice. The female mice in this study are post-menopausal, which means they have reduced levels of estrogen, resulting in metabolic syndrome and abnormal mitochondrial function. This phenomenon may contribute to the mitochondrial dysfunction present in our overweight, diabetic, and old Tg-Neg female mice. Therefore, an over-expression of caveolin-3 may be enhancing the localization of ERa to the plasma membrane in elderly female mice for better glucose regulation. It would be of interest to further examine the direct relationship between Cav3 and ER signaling in our old female diabetic mice.

This study suggests that the overexpression of Cav3 in the heart may limit injuries from metabolic syndrome and mitochondrial dysfunction. However, this study can be extended to understand the underlying pathway to explain the protective effects of Cav3 OE in this diabetic mouse model. Caveolins are involved in intricate signaling pathways

which will require deeper understanding. Therefore, I propose to perform RNA sequencing to identify changes in RNA expression levels between our control and diabetic groups and transgene-negative and caveolin-3 overexpressing mice. RNA sequencing will be beneficial in detecting functioning or non-functioning genes to explain the role of caveolin-3 in the diabetic heart. The RNA sequencing data can then be coupled with other biochemical assays to further analyze gene expression.

In conclusion, the male T2DM mice presented (i) metabolic syndrome from obesity and altered blood glucose tolerance; (ii) cardiomyopathy indicated by hypertrophy and diastolic dysfunction; (iii) and disrupted cardiomyocyte mitochondria ultrastructure. In males, cardiac specific overexpression of caveolin-3 protected from cardiac hypertrophy and diastolic dysfunction and preserved mitochondrial ultrastructure in diabetic mice. Likewise, the female T2DM mice also presented (i) metabolic syndrome; (ii) cardiomyopathy indicated by hypertrophy; (iii) abnormal mitochondrial function; and (iv) disrupted cardiomyocyte mitochondria ultrastructure. In females, cardiac specific overexpression of caveolin-3 protected from cardiac hypertrophy and preserved mitochondrial function and ultrastructure in diabetic mice. Overall, these findings implicate that research in sex differences is required to protect aging women and find anti-obesity and anti-diabetes therapies to improve women's long-term health. This study also confirms the regulatory role of caveolin-3 in age-related and diabetes-induced metabolic injury and cardiomyopathy. Targeting caveolin-3 may be a novel therapy for protecting a type 2 diabetic heart for both males and females.
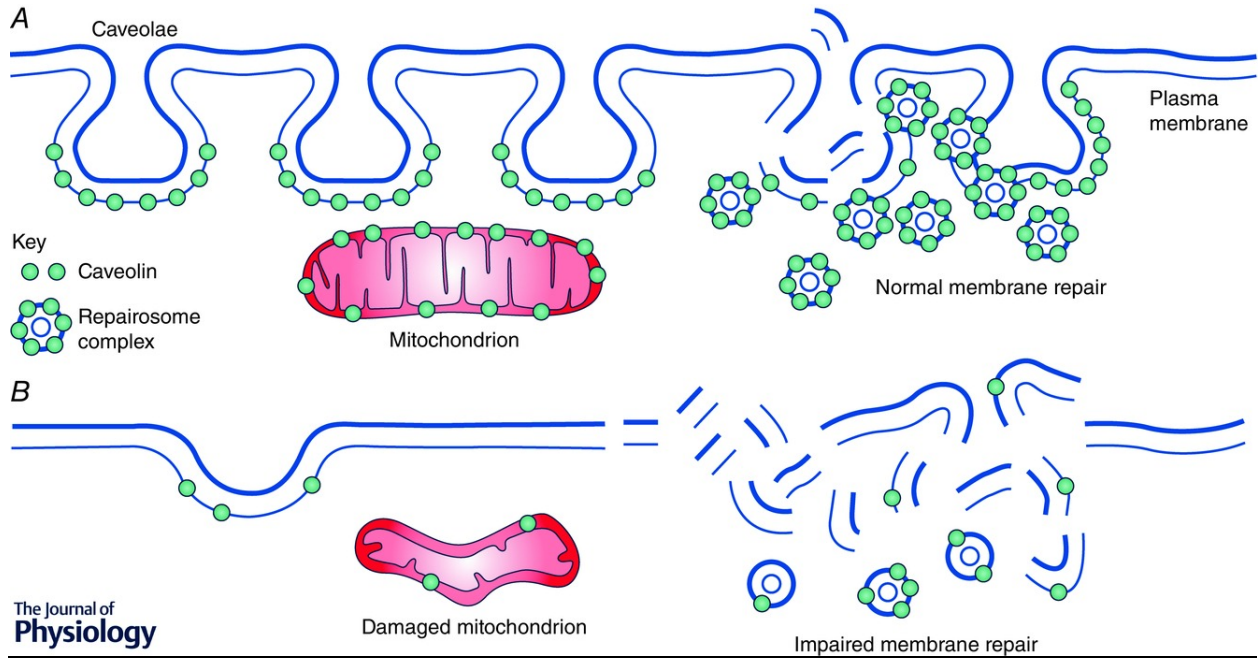
Figure 1: Caveolin localization within the plasma membrane and mitochondria may play a role in regulating membrane ultrastructure and mitochondrial function. Caveolin-3 is a structural protein that is present in striated muscle types, such as skeletal tissue and cardiac muscle. Image adapted from Schilling and Patel, 2016.
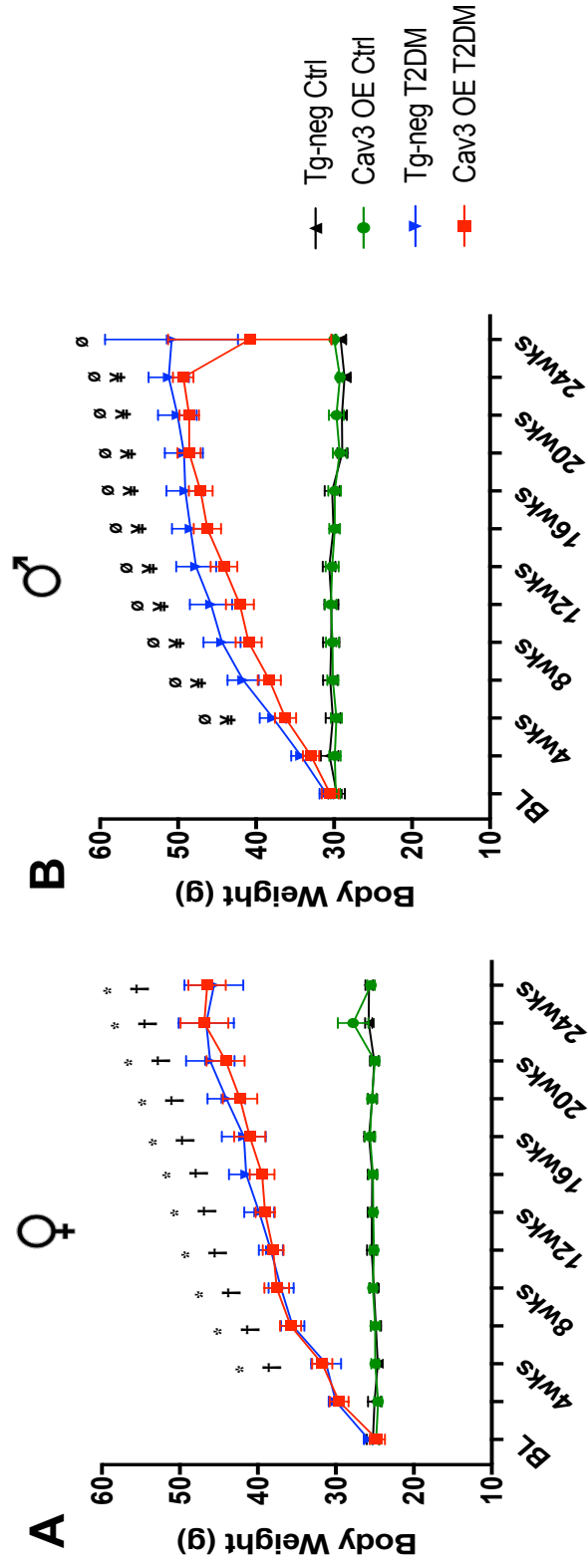
Figure 2: Streptozotocin and high-fat diet increased body weight of mid-aged female and male mice. Female and male Tg-Neg and Cav3 OE mice gained significant weight compared to the controls starting a 4 weeks post diabetes injection. Data are means $\pm$ SEM. Two-way ANOVA with Tukey multiple comparison tests were performed. $P<0.05$ female Tg-Neg Ctrl vs. female Cav3 OE Ctrl (#), female Tg-Neg Ctrl vs. female Tg-Neg T2DM (*), female Cav3 OE Ctrl vs. female Cav3 OE T2DM (+), female Tg-Neg T2DM vs. female Cav 3 OE T2DM (÷), male Tg-Neg Ctrl vs. male Cav3 OE Ctrl (¨), male Tg-Neg Ctrl vs. male Tg-Neg T2DM (ø), male Cav3 OE Ctrl vs. male Cav3 OE T2DM (¥), and male Tg-Neg T2DM vs. male Cav3 OE T2DM (≤).
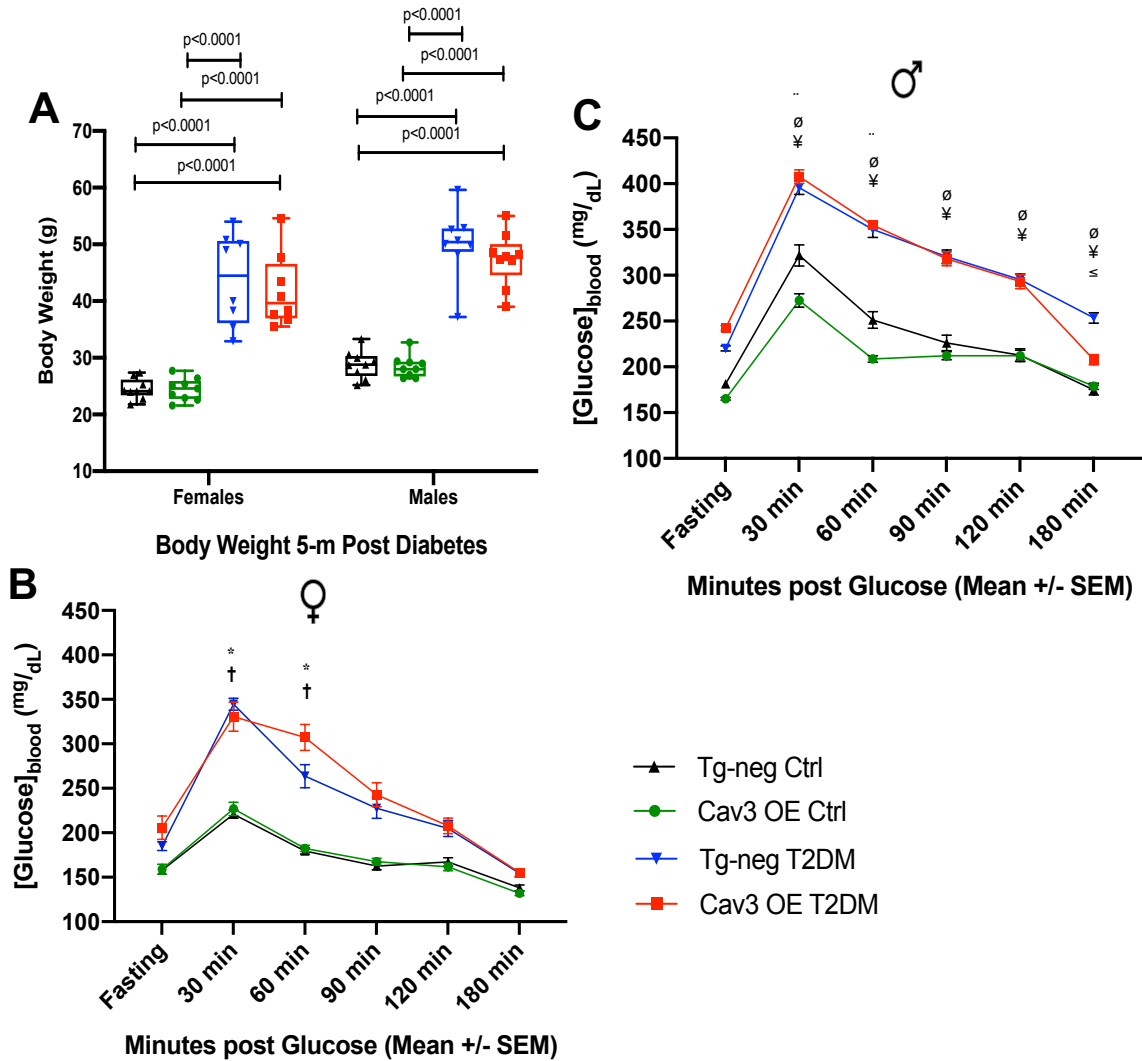
Figure 3: Streptozotocin injection and high-fat diet impaired glucose tolerance of female and male mice. Glucose tolerance test (GTT) was performed at 3-4 months post diabetes induction. A) Transgene-negative (Tg-Neg) and caveolin-3 overexpressing (Cav3 OE) type 2 diabetic (T2DM) mice had significantly greater body weights than controls at time of GTT. B) Female diabetic mice displayed altered glucose tolerance compared to the controls. C) Male diabetic mice showed worsened glycemic control compared to the controls. Data are means $\pm$ SEM. Two-way ANOVA with Tukey multiple comparison tests were performed. *P<0.05* female Tg-Neg Ctrl vs. female Cav3 OE Ctrl (**#**), female Tg-Neg Ctrl vs. female Tg-Neg T2DM (*****), female Cav3 OE Ctrl vs. female Cav3 OE T2DM (**†**), female Tg-Neg T2DM vs. female Cav 3 OE T2DM (÷), male Tg-Neg Ctrl vs. male Cav3 OE Ctrl (¨), male Tg-Neg Ctrl vs. male Tg-Neg T2DM (**ø**), male Cav3 OE Ctrl vs. male Cav3 OE T2DM (**¥**), and male Tg-Neg T2DM vs. male Cav3 OE T2DM (**≤**).

Table 1.1: Caveolin-3 overexpression protected female diabetic mice from cardiac hypertrophy. Echocardiogram measurements reveal that female Tg-Neg T2DM mice have larger hearts indicating cardiac hypertrophy, while Cav3 OE T2DM mice are protected. Systolic and diastolic function is preserved among all female groups. Data are means ± SEM. One-way ANOVA with Tukey multiple comparison tests were performed. P<0.05 vs. Tg-Neg Ctrl (*), vs. Cav3 OE Ctrl (†), vs. Tg-Neg T2DM (¥).

	Tg-Neg Ctrl	Cav3 OE Ctrl	Tg-Neg T2DM	Cav3 OE T2DM
Body Weight (g)	26.01 ± 0.67	25.58 ± 0.73	**48.33 ± 4.13** *** p<0.0001**	**49.18 ± 2.29** **† p<0.0001**
IVSd (mm) (Interventricular septal end diastole)	0.77 ± 0.02	0.78 ± 0.01	**0.96 ± 0.04** *** p<0.0001**	**0.85 ± 0.01** **¥ p=0.0263**
LVIDd (mm) (Left ventricular internal diameter end diastole)	3.09 ± 0.06	3.09 ± 0.13	3.31 ± 0.15	3.22 ± 0.10
LVPWd (mm) (Left ventricular posterior wall end diastole)	0.76 ± 0.02	0.78 ± 0.01	**0.96 ± 0.04** *** p<0.0001**	**0.85 ± 0.01** **¥ p=0.0266**
IVSs (mm) (interventricular septal end systole)	1.21 ± 0.03	1.24 ± 0.03	**1.40 ± 0.05** *** p=0.0080**	1.28 ± 0.04
LVIDs (mm) (Left ventricular internal diameter end systole)	1.88 ± 0.14	1.85 ± 0.10	2.18 ± 0.13	2.02 ± 0.08
LVPWs (mm) (Left ventricular posterior wall end systole)	1.19 ±. 04	1.22 ± 0.03	**1.35 ± 0.04** *** p=0.0123**	1.27 ± 0.02
%EF (Ejection fraction)	70.45 ± 4.14	72.38 ± 1.72	64.36 ± 1.98	68.54 ± 1.82
%FS (Fractional shortening)	39.61 ± 3.70	40.36 ± 1.42	34.23 ± 1.39	37.33 ± 1.48
LV Mass (mg) (Left ventricle mass)	73.30 ± 3.99	76.21 ± 6.27	**113.70 ± 11.28** *** p=0.0026**	90.89 ± 3.51
LV mass corrected (mg)	58.64 ± 3.196	60.97 ± 5.02	**90.96 ± 9.02** *** p=0.0026**	72.71 ± 2.81
MV E (mm/sec) (mitral valve flow E wave velocity)	600.97 ± 58.28	536.72 ± 40.44	675.67 ± 58.67	**741.64 ± 28.15** **† p=0.2229**
MV A (mm/sec) (mitral valve flow A wave velocity)	387.19 ± 18.74	345.96 ± 35.30	386.59 ± 75.48	457.17 ± 51.49
MV Deceleration acceleration (cm/sec^2)	-37161.83 ± 4152.76	-29880.15 ± 3079.14	-38305.96 ± 5476.96	-44843.80 ± 4926.42
MV Deceleration time (sec)	17.82 ± 1.04	18.83 ± 1.07	18.06 ± 1.03	18.61 ± 2.44
MV E / A	1.56 ± 0.15	1.60 ± 0.10	1.48 ± 0.23	1.96 ± 0.41
Ao-ET (msec) (aortic ejection time)	42.20 ± 1.61	41.81 ± 1.42	43.15 ± 1.28	39.17 ± 1.06
E' (mm/sec) (Peak velocity of early diastolic mitral annular motion)	-25.90 ± 1.69	-26.67 ± 2.43	-26.44 ± 3.37	-28.50 ± 3.23
A' (mm/sec) (Peak velocity of diastolic mitral annular motion)	-17.83 ± 2.16	-20.37 ± 3.84	-20.51 ± 1.44	-20.51 ± 2.32
E'/A'	1.50 ± 0.08	1.61 ± 0.24	1.28 ± 0.12	1.47 ± 0.20
A'/E'	0.68 ± 0.04	0.84 ± 0.24	0.82 ± 0.07	0.78 ± 0.14
MV E / E' (Left ventricle filling pressure)	-24.56 ± 3.83	-21.85 ± 2.80	-25.55 ± 2.81	-25.42 ± 3.64

Table 1.2: Caveolin-3 overexpression protected male diabetic mice from cardiac hypertrophy and preserved diastolic function. Echocardiogram measurements reveal that male Tg-Neg T2DM mice have larger hearts compared to Cav3 OE T2DM mice indicating cardiac hypertrophy. Systolic was preserved among all male mice, while diastolic dysfunction was observed in Tg-Neg T2DM mice. Data are means ± SEM. One-way ANOVA with Tukey multiple comparison tests were performed. P<0.05 vs. Tg-Neg Ctrl (*), vs. Cav3 OE Ctrl (†), vs. Tg-Neg T2DM (¥).

	Tg-Neg Ctrl	Cav3 OE Ctrl	Tg-Neg T2DM	Cav3 OE T2DM
Body Weight (g)	30.45 ± 0.78	29.68 ± 0.74	**50.90 ± 2.61 * p<0.0001**	**49.58 ± 1.42 † p<0.0001**
IVSd (mm) (Interventricular septal end diastole)	0.87 ± 0.01	0.80 ± 0.01	**0.99 ± 0.04 * p=0.0082**	0.89 ± 0.03
LVIDd (mm) (Left ventricular internal diameter end diastole)	3.28 ± 0.11	3.50 ± 0.06	3.56 ± 0.10	3.63 ± 0.10
LVPWd (mm) (Left ventricular posterior wall end diastole)	0.86 ± 0.01	0.81 ± 0.01	**0.98 ± 0.03 * p=0.0049**	**0.87 ± 0.02 ¥ p=0.0083**
IVSs (mm) (interventricular septal end systole)	1.25 ± 0.03	1.28 ± 0.02	1.37 ± 0.05	1.39 ± 0.03
LVIDs (mm) (Left ventricular internal diameter end systole)	2.31 ± 0.08	2.22 ± 0.06	2.48 ± 0.09	2.35 ± 0.13
LVPWs (mm) (Left ventricular posterior wall end systole)	1.22 ± 0.03	1.26 ± 0.02	1.37 ± 0.04	1.36 ± 0.05
%EF (Ejection fraction)	57.32 ± 2.57	66.40 ± 1.98	59.24 ± 2.81	65.51 ± 2.97
%FS (Fractional shortening)	29.40 ± 1.69	36.00 ± 1.47	30.96 ± 1.90	35.62 ± 2.16
LV Mass (mg) (Left ventricle mass)	95.74 ± 4.51	97.67 ± 2.73	**128.38 ± 9.05 * p=0.0108**	115.68 ± 7.94
LV mass corrected (mg)	76.59 ± 3.61	76.46 ± 1.62	**105.50 ± 7.58 * p=0.0053**	92.55 ± 6.35
MV E (mm/sec) (mitral valve flow E wave velocity)	836.91 ± 138.70	767.07 ± 101.87	925.87 ± 116.86	727.96 ± 72.26
MV A (mm/sec) (mitral valve flow A wave velocity)	630.10 ± 146.10	326.51 ± 49.46	700.33 ± 86.76	469.59 ± 56.39
MV Deceleration acceleration (cm/sec^2)	-54290.34 ± 11569.8	-32945.96 ± 2741.12	-54220.40 ± 8235.14	-42981.62 ± 7359.28
MV Deceleration time (sec)	17.66 ± 2.32	21.37 ± 1.46	18.94 ± 1.85	20.83 ± 2.64
MV E / A	1.34 ± 0.05	2.24 ± 0.41	1.40 ± 0.04	1.88 ± 0.38
AO-ET (msec) (aortic ejection time)	42.87 ± 0.97	39.11 ± 1.38	40.56 ± 0.73	39.80 ± 1.06
E' (mm/sec) (Peak velocity of early diastolic mitral annular motion)	-30.31 ± 2.83	-24.67 ± 2.65	**-18.63 ± 2.94 * p=0.0481**	-19.27 ± 2.91
A' (mm/sec) (Peak velocity of diastolic mitral annular motion)	-18.35 ± 2.32	-16.97 ± 1.69	-21.40 ± 3.52	-16.47 ± 2.20
E'/A'	1.76 ± 0.19	1.50 ± 0.21	1.12 ± 0.30	1.39 ± 0.24
A'/E'	0.61 ± 0.06	0.86 ± 0.22	1.43 ± 0.34	1.14 ± 0.31
MV E / E' (Left ventricle filling pressure)	-28.95 ± 4.88	-32.04 ± 3.09	**-57.48 ± 4.91 * p=0.0014**	-42.07 ± 4.69

Table 2.1: Heart, lung, and liver mass increased in diabetic female mice. Post-sacrifice, the female T2DM mice showed increased body weight and liver weight compared to the controls. Only Tg-Neg T2DM mice presented increased heart and lung weight compared to the controls. Cav3 OE T2DM mice are protected from heart and lung enlargement. Data are means ± SEM. One-way ANOVA with Tukey multiple comparison tests were performed. P<0.05 vs. Tg-Neg Ctrl (*), vs. Cav3 OE Ctrl (†), vs. Tg-Neg T2DM (¥).

	Tg-Neg Ctrl	Cav3 OE Ctrl	Tg-Neg T2DM	Cav3 OE T2DM
Body Weight (g)	25.86 ± 0.54	25.39 ± 0.56	**48.38 ± 4.92 * p<0.0001**	**47.45 ± 2.47 † p<0.0001**
Heart / tibia (mg/mm)	7.16 ± 0.22	6.75 ± 0.32	**9.85 ± 0.67 * p=0.0002**	**8.12 ± 0.30 ¥ p=0.0276**
Lung / tibia (mg/mm)	8.51 ± 0.21	8.61 ± 0.18	**10.16 ± 0.42 * p=0.0220**	9.16 ± 0.64
Liver / tibia (mg/mm)	69.13 ± 2.29	64.80 ± 3.08	**84.52 ± 5.54 * p=0.0266**	**81.43 ± 3.78 † p=0.0222**

Table 2.2: Heart and liver mass increased in diabetic male mice. Post-sacrifice, the male T2DM mice show increased body weight. In Tg-Neg T2DM mice only, the heart and liver weight increased significantly compared to the controls. The male Cav3 OE T2DM mice were protected from heart and liver enlargement. Data are means ± SEM. One-way ANOVA with Tukey multiple comparison tests were performed. P<0.05 vs. Tg-Neg Ctrl (*), vs. Cav3 OE Ctrl (†), vs. Tg-Neg T2DM (¥).

	Tg-Neg Ctrl	Cav3 OE Ctrl	Tg-Neg T2DM	Cav3 OE T2DM
Body Weight (g)	30.54 ± 0.65	29.19 ± 0.88	**49.73 ± 3.20 * p<0.0001**	**49.00 ± 1.51 † p<0.0001**
Heart weight/tibia (mg/mm)	9.08 ± 0.26	9.02 ± 0.45	**11.91 ± 0.73 * p=0.0032**	10.57 ± 0.60
Lung / tibia (mg/mm)	9.38 ± 0.35	10.15 ± 0.98	10.48 ± 0.30	9.37 ± 0.38
Liver / tibia (mg/mm)	74.85 ± 2.90	76.61 ± 5.79	**134.24 ± 23.46 * p=0.0052**	113.56 ± 7.62
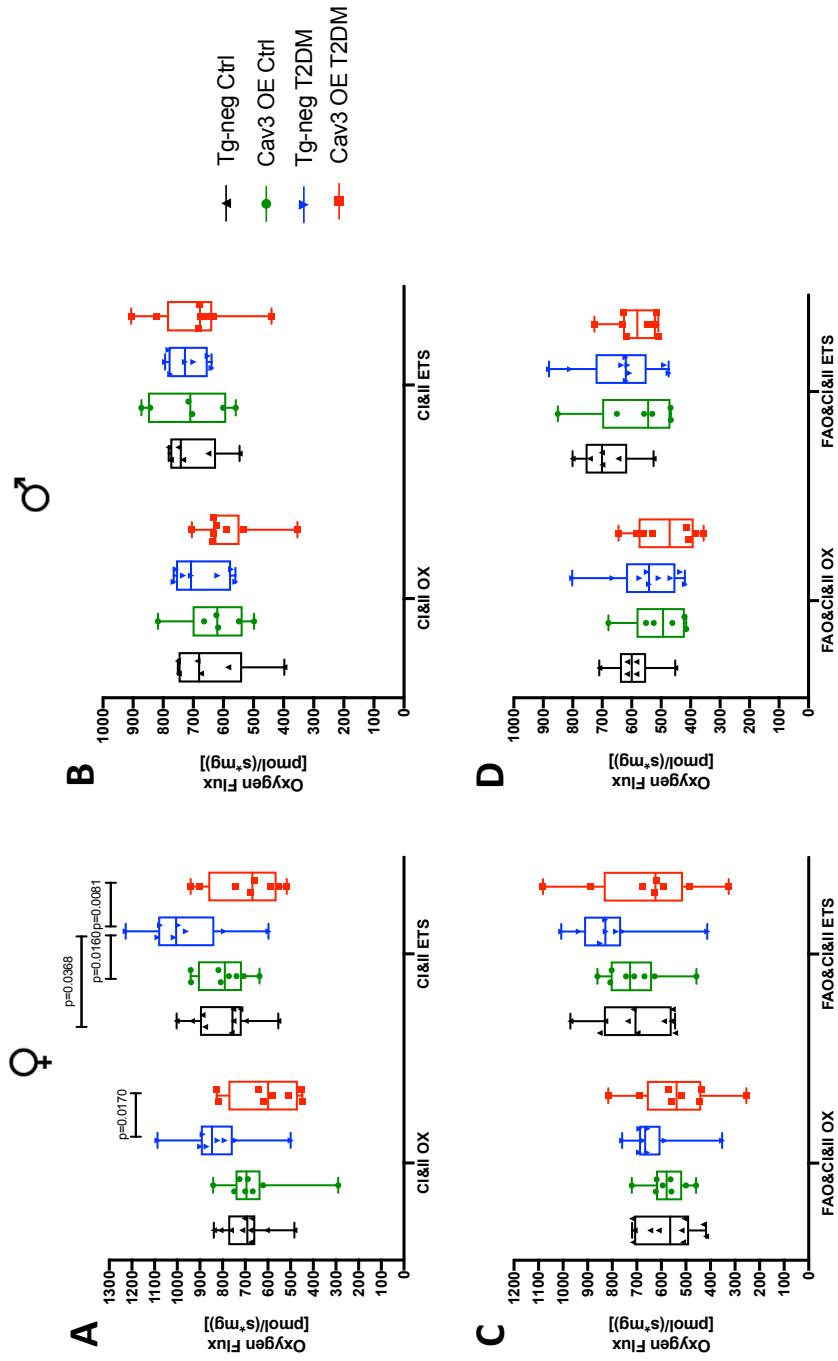
Figure 4: Caveolin-3 overexpression preserved mitochondrial function in female diabetic mice. Tg-Neg female diabetic mice display increased oxygen flux after the addition of Complex I & II substrates for oxidative phosphorylation. Fatty acid oxidation rates are not affected in females. Males do not present altered mitochondrial respiration during oxidative phosphorylation or fatty acid oxidation. Two-way ANOVA with Tukey multiple comparison tests were performed.
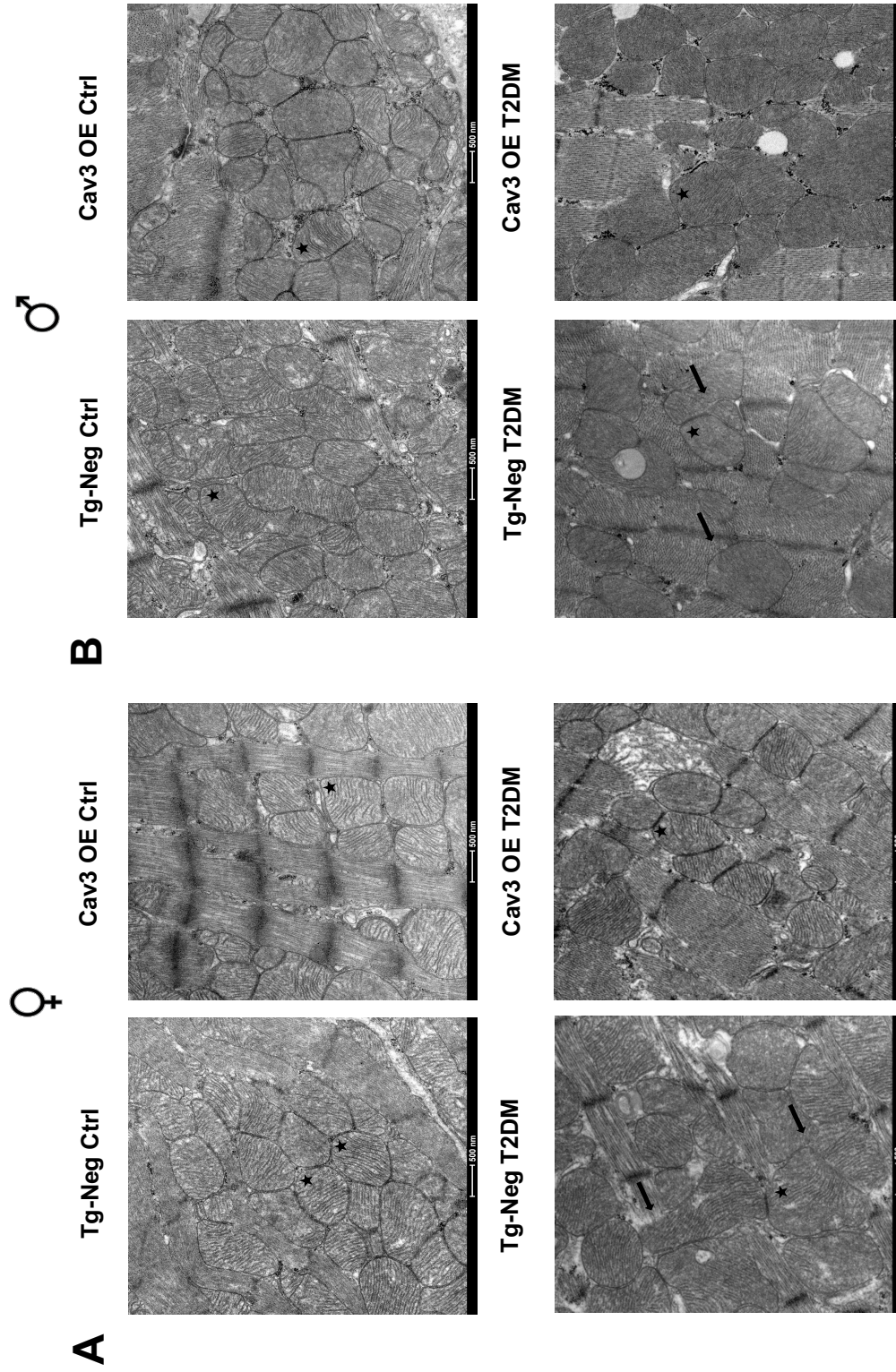
Figure 5: Caveolin-3 overexpression preserved membrane integrity and mitochondria size and connectivity in cardiomyocytes of diabetic mice. Diabetes induced mitochondrial disarray in A) females and B) males. Stars indicate examples of mitochondria. Arrows indicate disrupted mitochondria of interest. Images were taken at 9300x magnification.

REFERENCES

Abdullah, A., Peeters, A., de Courten, M., & Stoelwinder, J. (2010). The magnitude of association between overweight and obesity and the risk of diabetes: A meta-analysis of prospective cohort studies. *Diabetes Research and Clinical Practice*, *89*(3), 309–319. https://doi.org/10.1016/j.diabres.2010.04.012

Association, A. D. (2010). Diagnosis and Classification of Diabetes Mellitus. *Diabetes Care*, *33*(Suppl 1), S62-69. https://doi.org/10.2337/dc10-S062

Association, A. D. (2014). Standards of medical care in diabetes-2014. In *Diabetes Care* (Vol. 37). https://doi.org/10.2337/dc14-S014

Atkinson, M. A., Eisenbarth, G. S., & Michels, A. W. (2014). Type 1 diabetes. *The Lancet*, Vol. 383, pp. 69–82. https://doi.org/10.1016/S0140-6736(13)60591-7

Barros, R. P. A., Machado, U. F., & Gustafsson, J. Å. (2006). Estrogen receptors: new players in diabetes mellitus. *Trends in Molecular Medicine*, Vol. 12, pp. 425–431. https://doi.org/10.1016/j.molmed.2006.07.004

Battiprolu, P. K., Gillette, T. G., Wang, Z. V., Lavandero, S., & Hill, J. A. (2010). Diabetic cardiomyopathy: Mechanisms and therapeutic targets. *Drug Discovery Today: Disease Mechanisms*, Vol. 7. https://doi.org/10.1016/j.ddmec.2010.08.001

Berg, J. M., Tymoczko, J. L., & Stryer, L. (2002). *Oxidative Phosphorylation*.

Bordicchia, M., Liu, D., Amri, E. Z., Ailhaud, G., Dessì-Fulgheri, P., Zhang, C., Takahashi, N., Sarzani, R., & Collins, S. (2012). Cardiac natriuretic peptides act via p38 MAPK to induce the brown fat thermogenic program in mouse and human adipocytes. *Journal of Clinical Investigation*, *122*(3), 1022–1036. https://doi.org/10.1172/JCI59701

Borghetti, G., Von Lewinski, D., Eaton, D. M., Sourij, H., Houser, S. R., & Wallner, M. (2018). Diabetic cardiomyopathy: Current and future therapies. Beyond glycemic control. *Frontiers in Physiology*, Vol. 9. https://doi.org/10.3389/fphys.2018.01514

Boudina, S., & Abel, E. D. (2010). Diabetic cardiomyopathy, causes and effects. *Reviews in Endocrine and Metabolic Disorders*, Vol. 11, pp. 31–39. https://doi.org/10.1007/s11154-010-9131-7

Bugger, H., & Dale Abel, E. (2010). Mitochondria in the diabetic heart. *European Society of Cardiology*, *88*, 229–240. https://doi.org/10.1093/cvr/cvq239

Castagno, D., Baird-Gunning, J., Jhund, P. S., Biondi-Zoccai, G., MacDonald, M. R., Petrie, M. C., Gaita, F., & McMurray, J. J. V. (2011). Intensive glycemic control has no impact on the risk of heart failure in type 2 diabetic patients: Evidence from a

37,229 patient meta-analysis. *American Heart Journal*, *162*(5), 938-948.e2. https://doi.org/10.1016/j.ahj.2011.07.030

Chandramouli, C., Reichelt, M. E., Curl, C. L., Varma, U., Bienvenu, L. A., Koutsifeli, P., Raaijmakers A., De Blasio, M., Qin, C., Jenkins, A., Ritchie, R., Mellor, K., & Delbridge, L. M. D. (2018). Diastolic dysfunction is more apparent in STZ-induced diabetic female mice, despite less pronounced hyperglycemia. *Scientific Reports*, *8*(1), 1–13. https://doi.org/10.1038/s41598-018-20703-8

Chung, T. H., Wang, S. M., Liang, J. Y., Yang, S. H., & Wu, J. C. (2009). The interaction of estrogen receptor α and caveolin-3 regulates connexin43 phosphorylation in metabolic inhibition-treated rat cardiomyocytes. *International Journal of Biochemistry and Cell Biology*, *41*(11), 2323–2333. https://doi.org/10.1016/j.biocel.2009.06.001

Cogliati, S., Frezza, C., Soriano, M. E., Varanita, T., Quintana-Cabrera, R., Corrado, M., Cipolat, S., Costa, V., Casarin, A., Gomes, L., Perlas-Clemente, E., Salviati, L., Fernandez-Silva, P., Enriquez, J., & Scorrano, L. (2013). Mitochondrial cristae shape determines respiratory chain supercomplexes assembly and respiratory efficiency. *Cell*, *155*(1), 160–171. https://doi.org/10.1016/j.cell.2013.08.032

Curry, F. R. E. (2005). Atrial natriuretic peptide: An essential physiological regulator of transvascular fluid, protein transport, and plasma volume. *Journal of Clinical Investigation*, Vol. 115, pp. 1458–1461. https://doi.org/10.1172/JCI25417

Dandona, P., Aljada, A., & Bandyopadhyay, A. (2004). Inflammation: The link between insulin resistance, obesity and diabetes. *Trends in Immunology*, Vol. 25, pp. 4–7. https://doi.org/10.1016/j.it.2003.10.013

Dassanayaka, S., Readnower, R. D., Salabei, J. K., Long, B. W., Aird, A. L., Zheng, Y. T., Muthusamy, S., Facundo, H., Hill, B., & Jones, S. P. (2015). High glucose induces mitochondrial dysfunction independently of protein O-GlcNAcylation. *Biochemical Journal*, *467*(1), 115–126. https://doi.org/10.1042/BJ20141018

Ferko, M., Gvozdjaková, A., Kucharská, J., Mujkošová, J., Waczulíková, I., Styk, J., Ravingerova, T., Ziegelhoffer-Mihalovicova, B., & Ziegelhöffer, A. (2006). Functional Remodeling of Heart Mitochondria in Acute Diabetes: Interrelationships between Damage, Endogenous Protection and Adaptation. In *Gen. Physiol. Biophys* (Vol. 25).

Fonarow, G. C., & Hsu, J. J. (2016). Left Ventricular Ejection Fraction. *JACC: Heart Failure*, *4*(6), 511–513. https://doi.org/10.1016/j.jchf.2016.03.021 for Disease Control, C. (2017). *National Diabetes Statistics Report, 2017 Estimates of Diabetes and Its Burden in the United States Background*.

Fra, A. M., Williamson, E., Simons, K., & Parton, R. G. (1995). De novo formation of

caveolae in lymphocytes by expression of VIP21-caveolin. *Proceedings of the National Academy of Sciences of the United States of America*, *92*(19), 8655–8659. https://doi.org/10.1073/pnas.92.19.8655

Fridolfsson, H. N., Kawaraguchi, Y., Ali, S. S., Panneerselvam, M., Niesman, I. R., Finley, J. C., Kellerhals, S., Migita, M., Okada, H., Moreno, A., Jennings, M., Kidd, M., Bonds, J., Balijepalli, R., Ross, R., Patel, P., Miyanohara, A., Chen, Q., Lesnefsky, E., Head, B., Roth, D., Insel, P., & Patel, H. H. (2012). Mitochondria-localized caveolin in adaptation to cellular stress and injury. *FASEB Journal*, *26*(11), 4637–4649. https://doi.org/10.1096/fj.12-215798

Gnaiger, E. (2014). *Mitochondrial Pathways and Respiratory Control An Introduction to OXPHOS Analysis The Blue Book OROBOROS MiPNet Publications 2014*. Retrieved from www.bioblast.at/index.php/Gnaiger_2014_MitoPathways

Hales, C. M., Carroll, M. D., Fryar, C. D., & Ogden, C. L. (2015). *Prevalence of Obesity Among Adults and Youth: United States, 2015-2016 Key findings Data from the National Health and Nutrition Examination Survey*. Retrieved from https://www.cdc.gov/nchs/data/databriefs/db288_table.pdf#1.

Horikawa, Y. T., Panneerselvam, M., Kawaraguchi, Y., Tsutsumi, Y. M., Ali, S. S., Balijepalli, R. C., Murray, F., Head, B., Niesman, I., Rieg, T., Vallon, V., Insel, P., Patel, H., & Roth, D. M. (2011). Cardiac-specific overexpression of caveolin-3 attenuates cardiac hypertrophy and increases natriuretic peptide expression and signaling. *Journal of the American College of Cardiology*, *57*(22), 2273–2283. https://doi.org/10.1016/j.jacc.2010.12.032

Huxley, R., Barzi, F., & Woodward, M. (2006). Excess risk of fatal coronary heart disease associated with diabetes in men and women: Meta-analysis of 37 prospective cohort studies. *British Medical Journal*, Vol. 332, pp. 73–76. https://doi.org/10.1136/bmj.38678.389583.7C

Hyperglycemia in diabetes - Symptoms and causes - Mayo Clinic. (n.d.). Retrieved January 27, 2020, from https://www.mayoclinic.org/diseases-conditions/hyperglycemia/symptoms-causes/syc-20373631

International Diabetes Federation - Facts & figures. (n.d.). Retrieved November 15, 2019, from https://www.idf.org/aboutdiabetes/what-is-diabetes/facts-figures.html

Jia, G., Hill, M. A., & Sowers, J. R. (2018). Diabetic cardiomyopathy: An update of mechanisms contributing to this clinical entity. *Circulation Research*, Vol. 122, pp. 624–638. https://doi.org/10.1161/CIRCRESAHA.117.311586

Jujić, A., Nilsson, P. M., Engström, G., Hedblad, B., Melander, O., & Magnusson, M. (2014). Atrial natriuretic peptide and type 2 diabetes development - Biomarker and genotype association study. *PLoS ONE*, *9*(2), e89201.

https://doi.org/10.1371/journal.pone.0089201

Kahn, C. R. (1985). The Molecular Mechanism of Insulin Action. *Annual Review of Medicine*, *36*(1), 429–451. https://doi.org/10.1146/annurev.me.36.020185.002241

Kannel, W. B., & Wilson, P. W. (1995). Risk factors that attenuate the female coronary disease advantage. *Archives of Internal Medicine*, *155*(1), 57–61. Retrieved from http://www.ncbi.nlm.nih.gov/pubmed/7802521

Katakam, P. V. G., Jordan, J. E., Snipes, J. A., Tulbert, C. D., Miller, A. W., & Busija, D. W. (2007). Myocardial preconditioning against ischemia-reperfusion injury is abolished in Zucker obese rats with insulin resistance. *American Journal of Physiology-Regulatory, Integrative and Comparative Physiology*, *292*(2), R920–R926. https://doi.org/10.1152/ajpregu.00520.2006

Kavazis, A. N. (2015). Pathological vs. physiological cardiac hypertrophy. *Journal of Physiology*, Vol. 593, p. 3767. https://doi.org/10.1113/JP271161

Komatsu, M., Takei, M., Ishii, H., & Sato, Y. (2013). Glucose-stimulated insulin secretion: A newer perspective. *Journal of Diabetes Investigation*, Vol. 4, pp. 511–516. https://doi.org/10.1111/jdi.12094

Kühlbrandt, W. (2015). Structure and function of mitochondrial membrane protein complexes. *BMC Biology*, *13*(1), 89. https://doi.org/10.1186/s12915-015-0201-x

Leeners, B., Geary, N., Tobler, P. N., & Asarian, L. (2017). Ovarian hormones and obesity. *Human Reproduction Update*, *23*(3), 300–321. https://doi.org/10.1093/humupd/dmw045

Left ventricular hypertrophy - Symptoms and causes - Mayo Clinic. (n.d.). Retrieved January 29, 2020, from https://www.mayoclinic.org/diseases-conditions/left-ventricular-hypertrophy/symptoms-causes/syc-20374314

Legato, M. J., Gelzer, A., Goland, R., Ebner, S. A., Rajan, S., Villagra, V., & Kosowski, M. (2006). Gender-specific care of the patient with diabetes: Review and recommendations. *Gender Medicine*, *3*(2), 131–158. https://doi.org/10.1016/S1550-8579(06)80202-0

Lenzen, S. (2008). The mechanisms of alloxan- and streptozotocin-induced diabetes. *Diabetologia*, Vol. 51, pp. 216–226. https://doi.org/10.1007/s00125-007-0886-7

Levy, D., Anderson, K. M., Savage, D. D., Balkus, S. A., Kannel, W. B., & Castelli, W. P. (1987). Risk of ventricular arrhythmias in left ventricular hypertrophy: The Framingham Heart Study. *The American Journal of Cardiology*, *60*(7), 560–565. https://doi.org/10.1016/0002-9149(87)90305-5

Magnusson, M., Jujic, A., Hedblad, B., Engström, G., Persson, M., Struck, J., … Melander, O. (2012). Low plasma level of atrial natriuretic peptide predicts development of diabetes: The prospective Malmö diet and cancer study. *Journal of Clinical Endocrinology and Metabolism*, *97*(2), 638–645. https://doi.org/10.1210/jc.2011-2425

Marín-Peñalver, J. J., Martín-Timón, I., Sevillano-Collantes, C., & Cañizo-Gómez, F. J. del. (2016). Update on the treatment of type 2 diabetes mellitus. *World Journal of Diabetes*, *7*(17), 354. https://doi.org/10.4239/wjd.v7.i17.354

Maritim, A. C., Sanders, R. A., & Watkins, J. B. (2003). Diabetes, oxidative stress, and antioxidants: A review. *Journal of Biochemical and Molecular Toxicology*, *17*(1), 24–38. https://doi.org/10.1002/jbt.10058

Markandeya, Y. S., Phelan, L. J., Woon, M. T., Keefe, A. M., Reynolds, C. R., August, B. K., Hacker, T., Roth, D., Patel, H. H., & Balijepalli, R. C. (2015). Caveolin-3 overexpression attenuates cardiac hypertrophy via inhibition of T-type Ca2+ current modulated by protein kinase Cα in cardiomyocytes. *Journal of Biological Chemistry*, *290*(36), 22085–22100. https://doi.org/10.1074/jbc.M115.674945

Meyers, D. E., Basha, H. I., & Koenig, M. K. (2013). Mitochondrial cardiomyopathy: Pathophysiology, diagnosis, and management. *Texas Heart Institute Journal*, Vol. 40, pp. 385–394. Texas Heart Institute.

Mozaffarian, D., Benjamin, E. J., Go, A. S., Arnett, D. K., Blaha, M. J., Cushman, M., De Ferranti, S., Despres, J., Fullerton, H., Howard, V., Huffman, M., Judd, S., Kissela, B., Lackland, D., Lichtman, J., Lisabeth, L., Liu, S., Mackey, R., Matchar, D., McGuire, D., Mohler, E., Moy, C., Muntner, P., Mussolino, M., Nasir, K., Neumar, R., Nichol, G., Palaniappan, L., Pandey, D., Reeves, M., Rodriguez, C., Sorlie, P., Stein, J., Towfighi, A., Turan, T., Virani, S., Willey, J., Woo, D., Yeh, R., & Turner, M. B. (2015). Heart disease and stroke statistics-2015 update : A report from the American Heart Association. *Circulation*, *131*(4), e29–e39. https://doi.org/10.1161/CIR.0000000000000152

New CDC report: More than 100 million Americans have diabetes or prediabetes | CDC Online Newsroom | CDC. (n.d.). Retrieved November 15, 2019, from https://www.cdc.gov/media/releases/2017/p0718-diabetes-report.html

Nissen, S. E., & Wolski, K. (2007). Effect of rosiglitazone on the risk of myocardial infarction and death from cardiovascular causes. *New England Journal of Medicine*, *356*(24), 2457–2471. https://doi.org/10.1056/NEJMoa072761

Office of the Surgeon General (US). (n.d.). The Surgeon General's Call To Action To Prevent and Decrease Overweight and Obesity. Retrieved February 25, 2020, from https://www.ncbi.nlm.nih.gov/books/NBK44210/

Palade, G. (1953). Fine structure of blood capillaries. *J Appl Phys.*, *24*(1424).

Palicka, V. (2002). Pathophysiology of Diabetes Mellitus. *EJIFCC*, *13*(5), 140–144. Retrieved from http://www.ncbi.nlm.nih.gov/pubmed/30349429

Palmer, B. F., & Clegg, D. J. (2015). The sexual dimorphism of obesity. *Molecular and Cellular Endocrinology*, Vol. 402, pp. 113–119. https://doi.org/10.1016/j.mce.2014.11.029

Parikh, J., Zemljic-Harpf, A., Fu, J., Giamouridis, D., Hsieh, T. C., Kassan, A., Murthy, K., Bhargava, V., Patel, H. H., & Rajasekaran, M. R. (2017). Altered Penile Caveolin Expression in Diabetes: Potential Role in Erectile Dysfunction. *Journal of Sexual Medicine*, *14*(10), 1177–1186. https://doi.org/10.1016/j.jsxm.2017.08.006

Peters, S. A. E., Huxley, R. R., & Woodward, M. (2014). Diabetes as risk factor for incident coronary heart disease in women compared with men: A systematic review and meta-analysis of 64 cohorts including 858,507 individuals and 28,203 coronary events. *Diabetologia*, Vol. 57, pp. 1542–1551. https://doi.org/10.1007/s00125-014-3260-6

Pettersson, U. S., Waldén, T. B., Carlsson, P. O., Jansson, L., & Phillipson, M. (2012). Female Mice are Protected against High-Fat Diet Induced Metabolic Syndrome and Increase the Regulatory T Cell Population in Adipose Tissue. *PLoS ONE*, *7*(9). https://doi.org/10.1371/journal.pone.0046057

Picard, M., Shirihai, O. S., Gentil, B. J., & Burelle, Y. (2013). Mitochondrial morphology transitions and functions: Implications for retrograde signaling? *American Journal of Physiology - Regulatory Integrative and Comparative Physiology*, Vol. 304, p. R393. https://doi.org/10.1152/ajpregu.00584.2012

Raghavan, S., Vassy, J. L., Ho, Y.-L., Song, R. J., Gagnon, D. R., Cho, K., Wilson, P., & Phillips, L. S. (2019). Diabetes Mellitus-Related All-Cause and Cardiovascular Mortality in a National Cohort of Adults. *Journal of the American Heart Association*, *8*(4), e011295. https://doi.org/10.1161/JAHA.118.011295

Regitz-Zagrosek, V., Oertelt-Prigione, S., Prescott, E., Franconi, F., Gerdts, E., Foryst-Ludwig, A., Maas, A., Kautzky-Willer, A., Knappe-Wegner, D., Kintscher, U., Ladwig, K., Schenck-Gustafsson, K., & Stangl, V. (2016). Gender in cardiovascular diseases: Impact on clinical manifestations, management, and outcomes. *European Heart Journal*, *37*(1), 24–34. https://doi.org/10.1093/eurheartj/ehv598

Ribas, V., Drew, B. G., Zhou, Z., Phun, J., Kalajian, N. Y., Soleymani, T., Daraei, P., Widjaja, K., Wanagat, J., Vallim, T., Fluitt, A., Bensinger, S., Le, T., Radu, C., Whitelegge, J., Beaven S., Tontonoz, P., Lusis, A., Parks, B., Vergnes, L., Reur, K., Singh, H., Bopassa, J., Toro, L., Stefani, E., Watt, M., Schenk, S., Akerstrom, T., Kelly, M., Pedersen, B., Hewitt, S., Korach, K., & Hevener, A. L. (2016). Skeletal

muscle action of estrogen receptor a is critical for the maintenance of mitochondrial function and metabolic homeostasis in females. *Science Translational Medicine*, *8*(334). https://doi.org/10.1126/scitranslmed.aad3815

Ribas, V., Nguyen, M. T. A., Henstridge, D. C., Nguyen, A. K., Beaven, S. W., Watt, M. J., & Hevener, A. L. (2010). Impaired oxidative metabolism and inflammation are associated with insulin resistance in ERα-deficient mice. *American Journal of Physiology - Endocrinology and Metabolism*, *298*(2). https://doi.org/10.1152/ajpendo.00504.2009

Sargiacomo, M., Scherer, P. E., Tang, Z., Kübler, E., Song, K. S., Sanders, M. C., & Lisanti, M. P. (1995). Oligomeric structure of caveolin: Implications for caveolae membrane organization. *Proceedings of the National Academy of Sciences of the United States of America*, *92*(20), 9407–9411. https://doi.org/10.1073/pnas.92.20.9407

Schilling, J. M., & Patel, H. H. (2016). Non-canonical roles for caveolin in regulation of membrane repair and mitochondria: implications for stress adaptation with age. *The Journal of Physiology*, *594*(16), 4581–4589. https://doi.org/10.1113/JP270591

Shepherd, D. L., Hathaway, Q. A., Nichols, C. E., Durr, A. J., Pinti, M. V., Hughes, K. M., Kunovac, A., Stine, S., & Hollander, J. M. (2018). Mitochondrial proteome disruption in the diabetic heart through targeted epigenetic regulation at the mitochondrial heat shock protein 70 (mtHsp70) nuclear locus. *Journal of Molecular and Cellular Cardiology*, *119*, 104–115. https://doi.org/10.1016/j.yjmcc.2018.04.016

Skovsø, S. (2014). Modeling type 2 diabetes in rats using high fat diet and streptozotocin. *Journal of Diabetes Investigation*, Vol. 5, pp. 349–358. https://doi.org/10.1111/jdi.12235

Stachowiak, G., Pertyński, T., & Pertyńska-Marczewska, M. (2015). Metabolic disorders in menopause. *Przeglad Menopauzalny*, Vol. 14, pp. 59–64. https://doi.org/10.5114/pm.2015.50000

Strubbe, J. H., & Steffens, A. B. (1975). Rapid insulin release after ingestion of a meal in the unanesthetized rat. *American Journal of Physiology*, *229*(4), 1019–1022. https://doi.org/10.1152/ajplegacy.1975.229.4.1019

Tan, Z., Zhou, L. J., Mu, P. W., Liu, S. P., Chen, S. J., Fu, X. D., & Wang, T. H. (2012). Caveolin-3 is involved in the protection of resveratrol against high-fat-diet-induced insulin resistance by promoting GLUT4 translocation to the plasma membrane in skeletal muscle of ovariectomized rats. *Journal of Nutritional Biochemistry*, *23*(12), 1716–1724. https://doi.org/10.1016/j.jnutbio.2011.12.003

Tang, Z., Scherer, P. E., Okamoto, T., Song, K., Chu, C., Kohtz, D. S., Nishimoto, I., Lodish, H., & Lisanti, M. P. (1996). Molecular cloning of caveolin-3, a novel member

of the caveolin gene family expressed predominantly in muscle. *Journal of Biological Chemistry*, *271*(4), 2255–2261. https://doi.org/10.1074/jbc.271.4.2255

Ventura-Clapier, R., Garnier, A., Veksler, V., & Joubert, F. (2011). Bioenergetics of the failing heart. *Biochimica et Biophysica Acta - Molecular Cell Research*, Vol. 1813, pp. 1360–1372. https://doi.org/10.1016/j.bbamcr.2010.09.006

Wang, D., Gladysheva, I. P., Fan, T.-H. M., Sullivan, R., Houng, A. K., & Reed, G. L. (2014). Atrial natriuretic peptide affects cardiac remodeling, function, heart failure, and survival in a mouse model of dilated cardiomyopathy. *Hypertension (Dallas, Tex. : 1979)*, *63*(3), 514–519. https://doi.org/10.1161/HYPERTENSIONAHA.113.02164

Wilcox, G. (2005). Insulin and Insulin Resistance. In *Clin Biochem Rev* (Vol. 26).

Williams, T. M., & Lisanti, M. P. (2004). The caveolin proteins. *Genome Biology*, Vol. 5, p. 214. https://doi.org/10.1186/gb-2004-5-3-214

Witteles, R. M., & Fowler, M. B. (2008). Insulin-Resistant Cardiomyopathy. Clinical Evidence, Mechanisms, and Treatment Options. *Journal of the American College of Cardiology*, Vol. 51, pp. 93–102. https://doi.org/10.1016/j.jacc.2007.10.021

Woodman, S. E., Park, D. S., Cohen, A. W., Cheung, M. W. C., Chandra, M., Shirani, J., Tang, B., Jelicks, L., Kitsis, R., Christ, G., Factor, S., Tanowits, H., & Lisanti, M. P. (2002). Caveolin-3 knock-out mice develop a progressive cardiomyopathy and show hyperactivation of the p42/44 MAPK cascade. *Journal of Biological Chemistry*, *277*(41), 38988–38997. https://doi.org/10.1074/jbc.M205511200

Yamada, E. (1955). The fine structure of the gall bladder epithelium of the mouse. *The Journal of Biophysical and Biochemical Cytology*, *1*(5), 445–458. https://doi.org/10.1083/jcb.1.5.445

Yang, X. P., Liu, Y. H., Rhaleb, N. E., Kurihara, N., Kim, H. E., & Carretero, O. A. (1999). Echocardiographic assessment of cardiac function in conscious and anesthetized mice. *American Journal of Physiology - Heart and Circulatory Physiology*, *277*(5 46-5). https://doi.org/10.1152/ajpheart.1999.277.5.h1967

Yin, F. C., Spurgeon, H. A., Rakusan, K., Weisfeldt, M. L., & Lakatta, E. G. (1982). Use of tibial length to quantify cardiac hypertrophy: application in the aging rat. *The American Journal of Physiology*, *243*(6), H941-7. https://doi.org/10.1152/ajpheart.1982.243.6.H941

Zile, M. R., Gaasch, W. H., Carroll, J. D., Feldman, M. D., Aurigemma, G. P., Schaer, G. L., Ghali, J., & Liebson, P. R. (2001). Heart Failure With a Normal Ejection Fraction. *Circulation*, *104*(7), 779–782. https://doi.org/10.1161/hc3201.094226